Supplementary Information for:

Enhancing the capacity of supercapacitive swing adsorption CO_2 capture by tuning charging protocols

Trevor B. Binford, Grace Mapstone, Israel Temprano, Alexander C. Forse*

Experimental Methods

Device construction. Electrochemical gas adsorption experiments were carried out with a custom made device (Figure 1). A symmetric supercapacitor with 1 M NaCl (aq.) electrolyte was sandwiched between a bottom current collector and a titanium mesh contacting a top current collector, while the volume above the mesh was filled with pure CO_2 gas (Sigma Aldrich 99.9 atom% ^{12}C). A potentiostat (Biologic, VSP-3e) attached to the two current collectors applied a potential across the electrodes to charge the supercapacitor. By monitoring the gas reservoir with a pressure transducer (Omega, PX309-030A5V), we measured the CO_2 taken up or released by the SSA effect. Titanium was used for the current collectors and mesh to minimize corrosion. Chloride ions are particularly corrosive, so stainless steel is unsuitable for material in contact with the NaCl electrolyte.

Preparation of carbon films. All electrodes were made from activated carbon (YP-50F, Kuraray, which was found to perform favorably compared to activated carbons used in the literature) and polytetrafluoroethylene (PTFE, 60% wt. dispersion in water, Aldrich) mixed in a ratio of 95:5 by weight. The PTFE serves as a binder to hold together the electrode and make it more malleable for rolling out into a film. First, activated carbon was dispersed in several mL of ethanol in an ultrasonic bath, then mixed with the PTFE dispersion on a watch-glass. The mixture was continually stirred with a spatula to ensure through mixing. As the ethanol evaporated, drying portions of the mixture were gathered into a single mass, until enough ethanol evaporated that the collected carbon and PTFE had a dough-like consistency. After kneading and adding additional ethanol as necessary to achieve the desired consistency, the carbon was transferred to a glass sheet and rolled to a uniform thickness with a steel rolling pin. The material was then transferred with a razor blade to aluminum foil, which was folded into a wallet and placed into a vacuum oven overnight at 80-100 °C to remove residual ethanol/water.

After drying, circular electrodes were cut from the carbon film using a steel punch (0.5 inch diameter). Each electrode was cut to achieve a mass within 10% of 15 mg, and trimmed down if necessary (e.g. due to uneven film thickness). The mass of each electrode was recorded three times, with the mass recorded as the mean of the measurements and the error as the deviation from that mean. Filter paper (Whatman 55 mm Cat No. 1001-055) was used for a separator, cut into a circle slightly less than the diameter of the current collector. This minimized chances of a short circuit, such as from a misaligned electrode or bending titanium mesh contacting the opposite current collector.

Before assembly of the device, the electrodes were soaked to ensure good wetting and infiltration of the electrolyte into the activated carbon micropores. Either both electrodes (cells A1 and A2) or only the bottom electrode (cells B1 and B2) were soaked for 2 hours. In the case of the cells with only one soaked electrode, the soaked electrode was used in the bottom, non-gas exposed, side. For cells B1 and B2 the separator was soaked alongside the bottom electrode. For cells A1 and A2, the separator was only briefly soaked in electrolyte (for a few seconds) before assembly. Qualitatively similar results were obtained with both symmetric and asymmetric soaking (see figures and tables below).

Electrochemical gas adsorption experiments. The device was charged with a protocol adapted from Zhu et al.[1] A constant current (30 mA / g of the gas-exposed electrode) was applied until a target cell potential between the electrodes was reached. This potential was then held for 30 minutes (to give more time to equilibrate), then a 30 mA/g constant current applied to return the system to the initial potential, and a final 30 minute potential holding step. This procedure was repeated for the desired number of cycles.

For each charge/discharge cycle, the amount of CO_2 adsorbed was calculated by taking the difference between the peaks and troughs of the amount of gas in the reservoir. This was calculated from the pressure transducer data (smoothed over a window of 100 seconds) using the ideal gas equation $pV = nRT$. The volume of the reservoir was calculated during the process of dosing CO_2 into the cell, based on pressure measurements of the added gas (using Boyle's Law $P_1V_1 = P_2V_2$). The cell was kept in a 30 ºC incubator to control the temperature, though the initial temperature increase when first putting into the incubator is associated with the initial rise in the calculated amount of gas in the cell. To account for any linear changes in pressure over time each peak value was compared to the mean of the two adjacent troughs. The amount of gas adsorbed in one cycle was then normalized by the mass of carbon in the gas-exposed electrode to give the adsorption capacity in mmol/kg. The overall adsorption capacity was taken as the mean of adsorption capacities for each cycle, and the error calculated using a 95% confidence interval with the Student's t-test.

Although the calculated metrics were generally consistent from one cycle to the next (within ~10%), there were occasional outlier cycles. These are evident in the gas in reservoir vs time plots as deviations from a smooth, roughly sinusoidal curve. Such outliers are attributed to rapid changes in temperature (due to other activities in the lab) or intermittent leaks in the cell (caused by poor seals, perhaps from corrosion by electrolyte interaction with the metal of the cell). Any results from these cycles were excluded from the analysis above to calculate the reported data.

Supplementary Figures

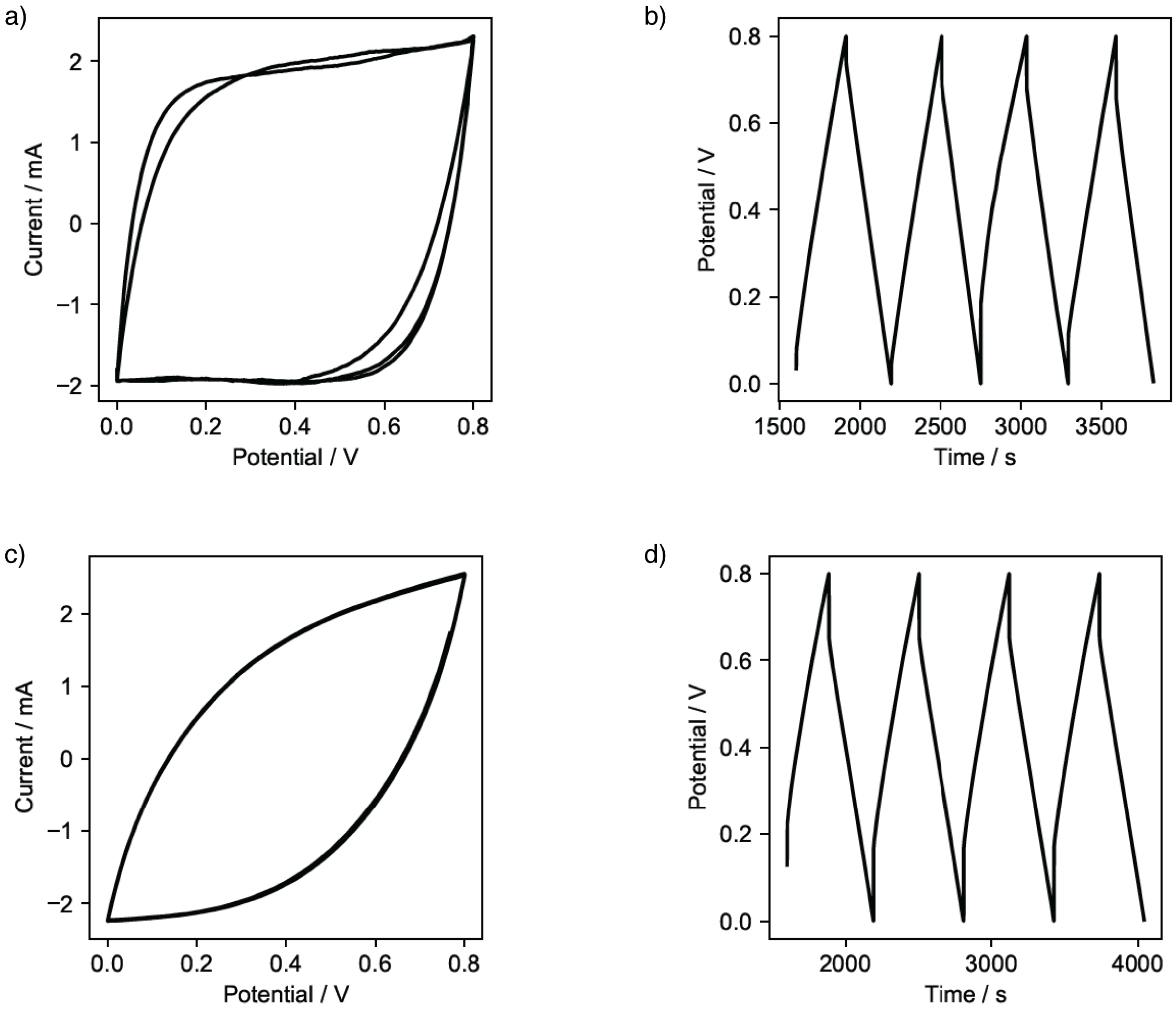

Figure S1. Initial electrochemical characterization of different activated carbons in coin cell supercapacitors. a) and b) Electrochemical data from coin cell made with 95 wt.% BPL carbon : 5 wt.% PTFE electrodes and 1 M NaCl electrolyte. a) cyclic voltammogram conducted between 0 V and 0.8 V with scan rate of 5 mV/s; b) constant current charge-discharge experiment conducted between 0 V and 0.8 V with current of 1 mA. c) and d) Electrochemical data from coin cell made with 95 wt. % YP-50F carbon : 5 wt.% PTFE electrodes and 1 M NaCl electrolyte. c) CV conducted between 0 V and 0.8 V with scan rate of 5 mV/s; d) constant current charge-discharge conducted between 0 V and 0.8 V with current of 1 mA. Analysis of the constant current charge-discharge data gave gravimetric capacitances of 53 ± 4 F/g and 67 ± 1 F/g, for BPL activated carbon and YP50-F activated carbon, respectively.

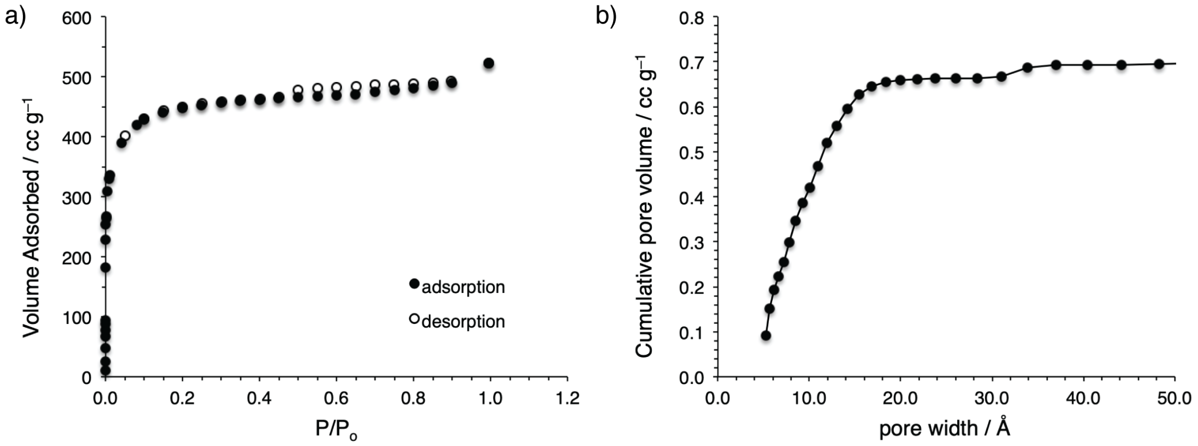

Figure S2. Gas sorption data and analysis for YP50-F activated carbon. a) 77 K N_2 sorption isotherm for YP50-F powder. Prior to analysis, the sample was washed extensively with water, dried, and finally activated under vacuum for 16 h at 120 ºC. The N_2 isotherm was then collected using an Anton Parr Autosorb iQ-XR instrument. A BET surface area of 1690 m^2 g^{-1} was obtained by using the BET equation and Rouquerol's consistency criteria, as implemented in AsiQwin software. b) Cumulative pore volume obtained using a quenched solid density functional theory (QSDFT) model (with carbon slit pores) as implemented in AsiQwin. The majority of the pores in this material have a pore width below 20 Å.

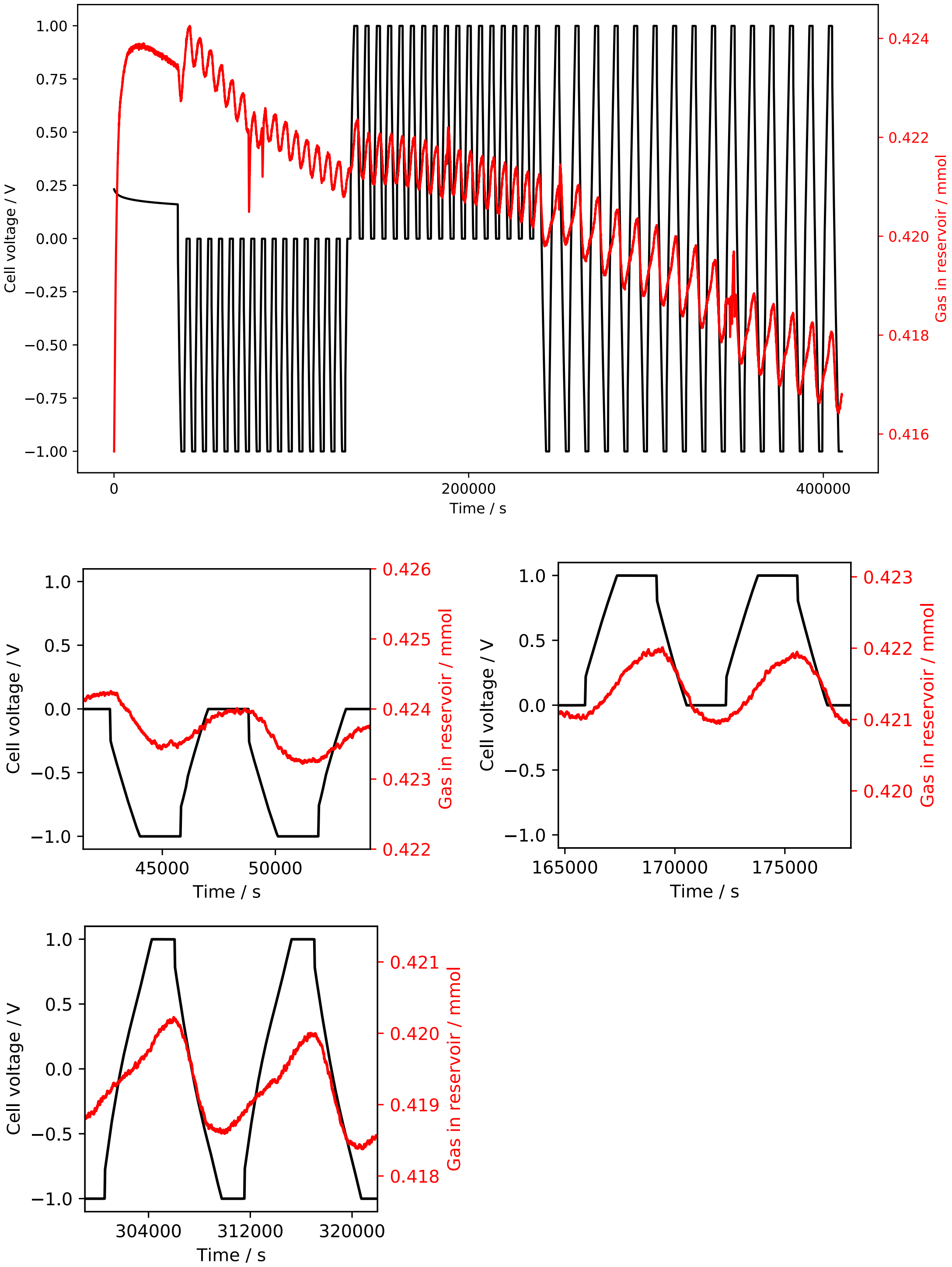

Figure S3. Overall experiment and representative cycles from positive, negative, and switching cycling protocols on cell A1 (same as in main body of this paper). Conducted with 1 M NaCl (aq) electrolyte, 15 mg electrodes, and 30 mA g^{-1} current density. Anomalous peaks are presumed to be from short-term temperature changes. In additional to the reversible adsorption, gradual irreversible pressure reductions are observed throughout the experiment, which may arise due to irreversible electrochemical processes such as corrosion. During the first part of the experiment, where the open circuit voltage was measured, initial pressure increases are observed as the cell thermalizes in the incubator oven. Subsequently, pressure decreases are observed due to chemical adsorption of CO_2 into the supercapacitor cell.

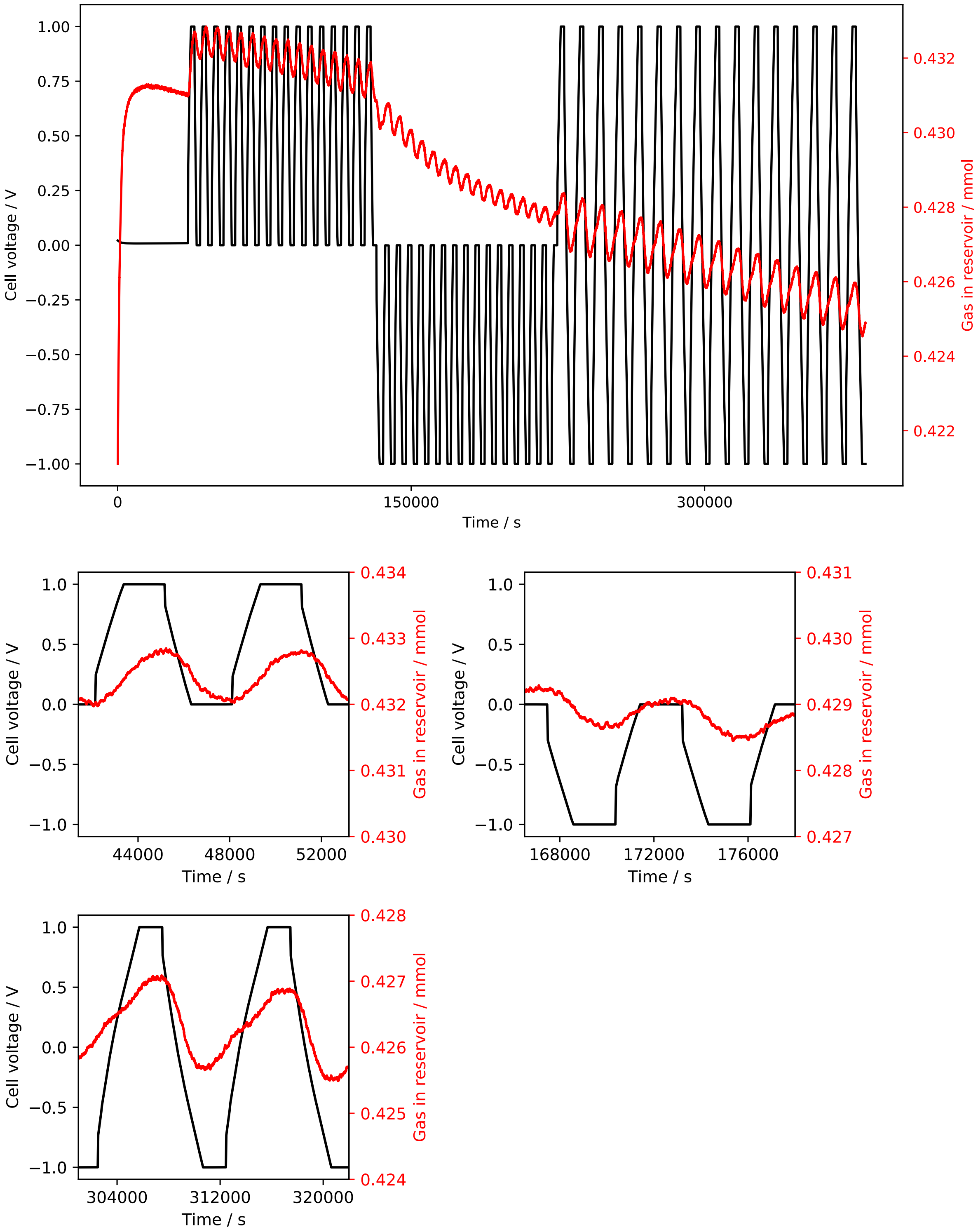

Figure S4. Overall experiment and representative cycles from negative, positive, and switching cycling protocols on cell A2. Conducted with 1 M NaCl (aq) electrolyte, 15 mg electrodes, and 30 mA g^{-1} current density. Anomalous peaks are presumed to be from short-term temperature changes. During the first part of the experiment, where the open circuit voltage was measured, initial pressure increases are observed as the cell thermalizes in the incubator oven. Subsequently, pressure decreases are observed due to chemical adsorption of CO_2 into the supercapacitor cell.

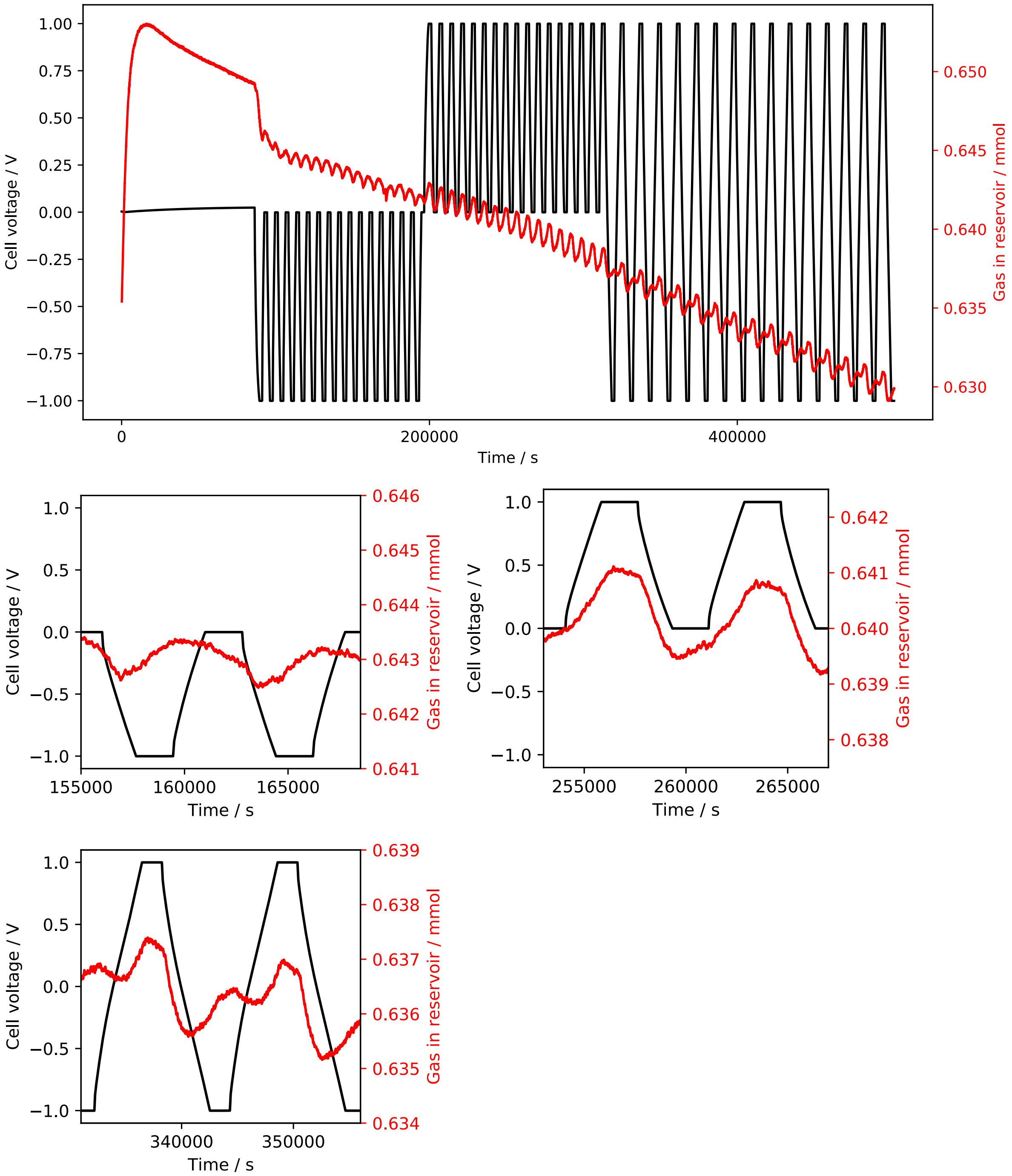

Figure S5. Overall experiment and representative cycles from negative, positive, and switching cycling protocols on cell B1. Conducted with 1 M NaCl (aq) electrolyte, 15 mg electrodes, and 30 mA g^{-1} current density. Anomalous peaks presumed to be from short-term temperature changes. As opposed to cells A1 and A2, only the electrode not directly exposed to the gas was soaked with electrolyte (the gas-exposed electrode was wetted with a few drops of electrolyte). During the first part of the experiment, where the open circuit voltage was measured, initial pressure increases are observed as the cell thermalizes in the incubator oven. Subsequently, pressure decreases are observed due to chemical adsorption of CO_2 into the supercapacitor cell.

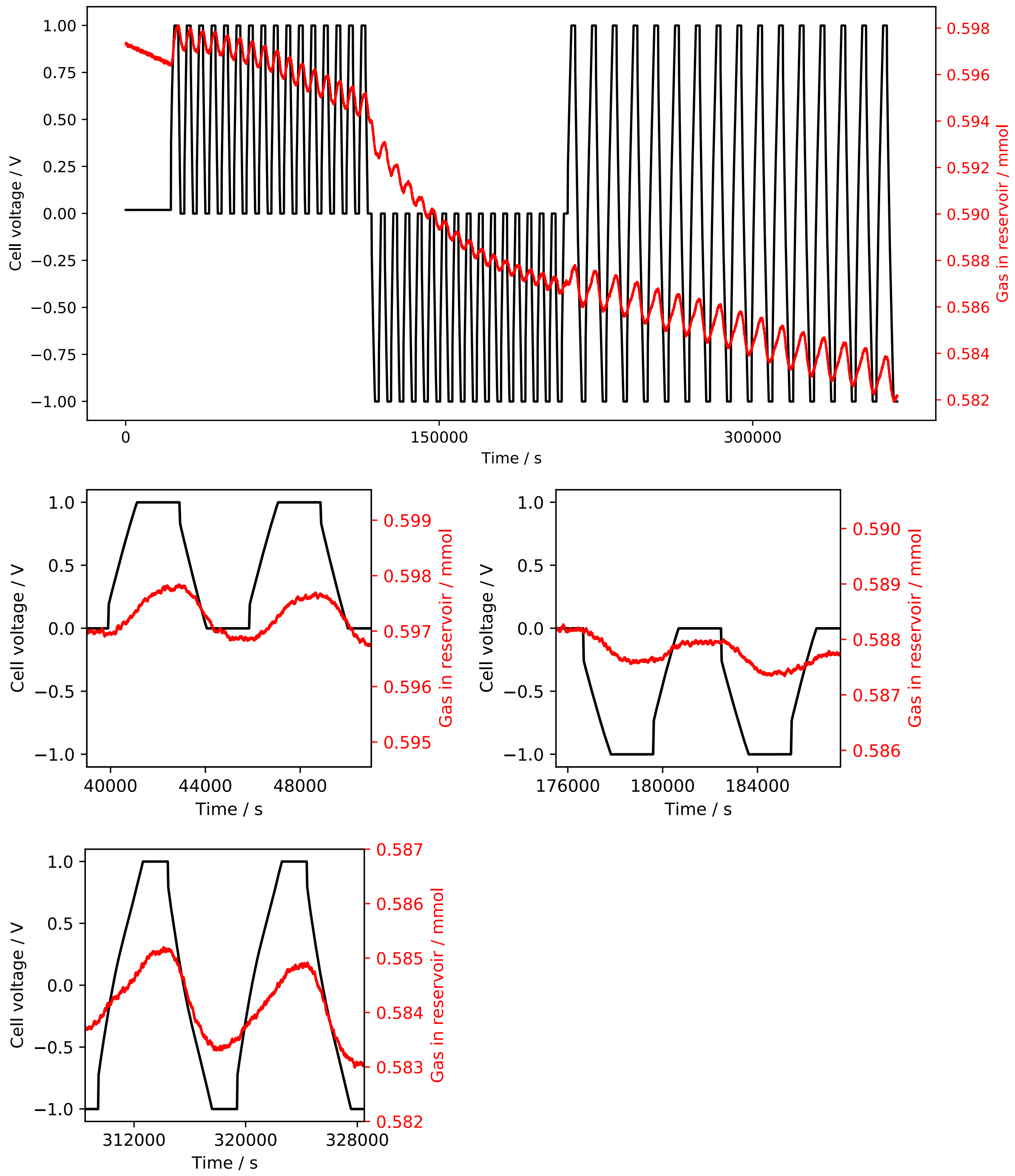

Figure S6. Overall experiment and representative cycles from positive, negative, and switching cycling protocols on cell B2. Conducted with 1 M NaCl (aq) electrolyte, 15 mg electrodes, and 30 mA g^{-1} current density. Anomalous peaks presumed to be from short-term temperature changes. As opposed to cells A1 and A2, only the electrode not directly exposed to the gas was soaked with electrolyte (the gas-exposed electrode was wetted with a few drops of electrolyte). During the first part of the experiment, where the open circuit voltage was measured, initial pressure increases are observed as the cell thermalizes in the incubator oven. Subsequently, pressure decreases are observed due to chemical adsorption of CO_2 into the supercapacitor cell.

Table S1. Adsorption capacities (in mmol kg^{-1}) and energy consumption (in kJ mol^{-1}) for literature data for comparison.[1] Data is for a supercapacitor with BPL 4 × 6 activated carbon electrodes and 1 M NaCl electrolyte. Measurements were carried out with a 15% CO_2 and 85% N_2 gas mixture, under flow through conditions. The charging protocol was the same as our negative charging protocol.

	Adsorption capacity / mmol kg^{-1}	Energy consumption / kJ mol^{-1}
Negative	62 ± 3	202 ± 14

Table S2. Adsorption capacities (in mmol kg^{-1}) and energy consumption (in kJ mol^{-1}) for two cells that were cycled with first a negative charging protocol, then positive, then switching. Each cell was assembled and run by a different researcher to minimize biases. Cell A1 had both electrodes soaked; cell B1 had only electrode not exposed to gas soaked.

Cell	A1		B1	
	Adsorption capacity / mmol kg^{-1}	Energy consumption / kJ mol^{-1}	Adsorption capacity / mmol kg^{-1}	Energy consumption / kJ mol^{-1}
Negative	50 ± 1	628 ± 12	55 ± 5	445 ± 85
Positive	75 ± 1	356 ± 17	108 ± 2	217 ± 22
Switching	112 ± 7	751 ± 39	111 ± 3	596 ± 48

Table S3. Adsorption capacities (in mmol kg^{-1}) and energy consumption (in kJ mol^{-1}) for two cells that were cycled with first a positive charging protocol, then negative, then switching. Each cell was assembled and run by a different researcher to minimize biases. Cell A2 had both electrodes soaked; cell B2 had only electrode not exposed to gas soaked.

Cell	A2		B2	
	Adsorption capacity / mmol kg^{-1}	Energy consumption / kJ mol^{-1}	Adsorption capacity / mmol kg^{-1}	Energy consumption / kJ mol^{-1}
Positive	66 ± 4	348 ± 27	75 ± 2	252 ± 14
Negative	38 ± 4	819 ± 47	48 ± 6	588 ± 43
Switching	97 ± 2	803 ± 20	123 ± 2	621 ± 12

References:

(1) Zhu, S.; Ma, K.; Landskron, K. *J. Phys. Chem. C* **2018**, *122*, 18476–18483.